Macromolecules **1996,** *29,* 713−717 **713**

Simple Integral Equation for the Polymer Brush

Henri Orland[†]

CEA, Service de Physique Théorique, CE-Saclay, 91191 Gif-sur-Yvette Cedex, France

M. Schick*

Department of Physics, University of Washington, Box 351560,
Seattle, Washington 98195-1560

Received June 16, 1995; Revised Manuscript Received October 2, 1995[⊗]

ABSTRACT: Employing a self-consistent mean field theory approach, we consider the density profile of a polymer brush. We express the self-consistent equation in terms of the monomer density and, by considering only a restricted set of polymer trajectories, reduce it to a relatively simple integral equation for the density profile. We find rather good agreement between the solution of our equation and that of the original one over almost the whole profile range. In particular, the profile reproduces well the smooth decay of the monomer density at the free surface of the brush and in this regard is an improvement over the classical parabolic profile.

The problem of calculating the density profile of a polymer brush in a solvent has received a great deal of attention and is now fairly well understood. One number which characterizes it is the brush height h, which is the first moment of the profile. The dependence of the height on the number of chains per unit area, σ, the polymerization index N, the excluded volume parameter w, and a Kuhn length a is obtained from scaling arguments[1,2] which balance the decrease in energy when the anchored polymers stretch to reduce their interactions, $N(w\sigma N/h)$, against the entropy lost when they do so, h^2/Na^2. This shows that the height of the brush, h, scales as $h \sim N(w\sigma a^2)^{1/3}$. The linear dependence on N, contrasted with the fractional power N^ν, $\nu < 1$, characteristic of a polymer melt or of a solution in good solvent, indicates that the polymers are strongly stretched. Experimental results are consistent with this scaling.[3] The argument does not give further information about the density profile.

More detailed information can be expected from the self-consistent field theory (SCFT),[4] which replaces the problem of many interacting polymers with that of a single polymer in a spatially-dependent external chemical potential. The latter is determined self-consistently from the local polymer density. The statistical mechanics of flexible polymers is, within this approximation, equivalent to the quantum mechanics of a particle moving in a potential proportional to the chemical potential. For large values of N, the usual methods[5,6] for solving the equivalent quantum problem become unwieldy because the number of equally important eigenstates is very large. The key to overcoming the difficulty was the observation by Semenov,[7] in a related context, that in the large-N limit, the quantum fluctuations about the classical path are small and can be neglected, so that the problem reduces to a classical one. In the polymer context, the diffusive excursions of a chain about its most probable path are small and can be neglected. This insight was applied to the brush by Milner, Witten, and Cates[8,9] and Zhulina and coworkers[10] and results in a density profile which is parabolic out to a distance at which the density vanishes. Beyond this distance, the density profile is identically zero.

For the most part, this approximation to the full SCFT is very successful. The profiles it provides agree well with those obtained from the SCFT applied to a system on a lattice and solved numerically without further approximation.[12] Monte Carlo[12,13] and molecular dynamics[14] simulations of moderately long polymers also show that the density profile is given rather well by a parabolic one as the polymerization index N increases. There are appreciable deviations, however, both near the wall and near the surface of the brush. A depletion zone occurs in the vicinity of the wall, so that the maximum of the density occurs some distance away from it. Near the outer surface of the brush, the profile decreases much more gradually and extends further out than in the parabolic approximation. This is understandable because at the outer edge, the polymers have the greatest freedom to make excursions about the most probable path, so that corrections to this path should be largest there.[15]

In this paper, we investigate an alternative method of solving approximately the full SCFT equations which shares much of the simplicity of those of refs 8 and 10 but yields a better approximation to the profile over its whole range. Before doing so, we briefly review the SCFT and its application to the polymer brush.

Our starting point is the partition function for a system of n polymers of polymerization index N grafted to a planar surface of unit area at $z = 0$. Provided that the grafting density is at least moderately high, $N\sigma a^2 \gg 1$, the problem of calculating the profile can be reduced to a one-dimensional one.[11] In this case, the partition function is

$$Z = \prod_{\alpha=1}^{n} \int Dz_\alpha \exp\left\{ -\frac{1}{2a^2}\int_0^N \mathrm{d}s\, [\dot{z}_\alpha(s)]^2 - \frac{w}{2}\int \mathrm{d}z\, \hat{\rho}^2(z) \right\} \tag{1}$$

where the functional integral is over all chain configurations $z(s)$ with $z(0) = z_0$ and $z(N) = 0$, w is the excluded volume parameter, a is the Kuhn length, and $\hat{\rho}(z)$ is the local density of monomers per unit length

---

[†] Also at Groupe de Physique Statistique, Université de Cergy-Pontoise, 95806 Cergy-Pontoise Cedex, France.

[⊗] Abstract published in *Advance ACS Abstracts,* December 15, 1995.

0024-9297/96/2229-0713$12.00/0 © 1996 American Chemical Society

$$\hat{\rho}(z) = \sum_{\alpha=1}^{n} \int_0^N \mathrm{d}s\, \delta(z - z_\alpha(s)) \qquad (2)$$

This partition function embodies several assumptions, among which are that the chains can be treated as being infinitely extensible and that their interaction with the solvent can be encompassed by a second virial coefficient. This latter assumption has been questioned by Carignano and Szleifer[16] and has been examined extensively by Martin and Wang,[17] who found it adequate if N is sufficiently large. It also assumes that the density profile is a function only of the coordinate measuring distances normal to the grafting surface, z. One now inserts the functional integral $\int D\phi\delta[\phi(z) - \hat{\rho}(z)] = 1$ into eq 1 so that all $\hat{\rho}(z)$, which depend on the chain configurations, can be replaced by $\phi(z)$, which do not. Then a standard integral representation, over the variable μ, of the delta function, is used, and the Gaussian integral over ϕ carried out with the result

$$Z = \mathcal{N} \int D\mu \exp\left\{\int \mathrm{d}z \frac{\mu^2(z)}{2w}\right\} Q^n[\mu] \qquad (3)$$

where $\mathcal{N}$ is an unimportant constant and $Q[\mu]$ is the partition function of a single chain in the external field $\mu(z)$,

$$Q[\mu] = \int Dz \exp\left\{-\int_0^N \mathrm{d}s \left[\frac{\dot{z}(s)^2}{2a^2} + \mu(z(s))\right]\right\} \qquad (4)$$

This representation of the original partition function is exact and replaces the interacting chain problem by one of independent chains subject to a fluctuating external field. The mean-field approximation consists in replacing this fluctuating field with a stationary one chosen such that its contribution to the partition function is maximal. The integrand of eq 3 is largest when

$$\begin{aligned} \mu(z) &= -\sigma w \frac{\partial \log Q[\mu]}{\partial \mu} \\ &\equiv \sigma w \rho(z) \end{aligned} \qquad (5)$$

where σ is the number of chains per unit area and $\rho(z)$ is the average value of the local density calculated in the ensemble of noninteracting chains subject to the external field μ. Equation 5 is the self-consistent equation for the field or, equivalently, for the density. It can be written explicitly as

$$\rho(y) = \frac{1}{Q} \int Dz \int_0^N \mathrm{d}s'\, \delta(y - z(s')) \exp\left\{-\int_0^N \mathrm{d}s \left[\frac{\dot{z}(s)^2}{2a^2} + w\sigma\rho(z(s))\right]\right\} \qquad (6)$$

The density is normalized such that

$$\int_0^\infty \rho(z)\, \mathrm{d}z = N \qquad (7)$$

This single self-consistent equation is not solved directly, but in two steps. First, the probability, $q(s,z)$, that a chain of s monomers in the field $\mu(z)$ has one end at z is obtained by solving the modified diffusion equation

$$\frac{\partial q(s,z)}{\partial s} = \frac{a^2}{2} \frac{\partial^2 q(s,z)}{\partial z^2} - \mu(z) q(s,z) \qquad (8)$$

From the propagator $q(s,z)$, the density is obtained according to

$$\rho(z) = \frac{\int_0^N \mathrm{d}s\, q(s,z) q(N-s,z)}{\int \mathrm{d}y\, q(N,y)} \qquad (9)$$

As the potential in eq 8 is related to the density itself, eqs 5, 8, and 9 constitute a set of three self-consistent equations for the density, external field, and propagator, which are equivalent to the single one of eq 6 for the density.

The problem is now solved, in principle, within the SCFT. Practical implementation can be laborious, of course. We have obtained numerical solutions of the self-consistent equations for various values of N and σw. A typical profile is shown in Figure 1 for $N = 100$ and $\sigma w = 0.1$.

The lengthy process of solving the set of SCFT equations can be simplified enormously when the chains are strongly stretched, as they are for the brush. In this case, Semenov[7] noted that the single-chain partition function, $Q(\mu)$, eq 4 is dominated by the chain configurations which take the most probable path, or classical path, given by

$$\frac{\ddot{z}(s)}{a^2} = \frac{\mathrm{d}\mu(z)}{\mathrm{d}z} \qquad (10)$$

That is, a good approximation to the solution of the self-consistent "quantum" problem, eq 8 above, is the solution of the classical problem eq 10. This equation is solved subject to the initial condition $\dot{z}(0) = 0$, as there is no force on the polymer at the free end, and final condition $z(N) = 0$. These conditions imply

$$N = \int_0^{z_0} \frac{\mathrm{d}z}{\{2a^2[\mu(z) - \mu(z_0)]\}^{1/2}} \qquad (11)$$

where $z_0 = z(0)$, the unknown initial position. Finally, as all polymers reach the grafting surface after N steps *irrespective* of their initial coordinate z_0, the value of N is independent of z_0:

$$\frac{\mathrm{d}N}{\mathrm{d}z_0} = 0 \qquad (12)$$

In the classical mechanics analog of eq 10, the potential must be such that all particles reach the origin at the same time irrespective of their starting position. Such a potential is, of course, parabolic. As the monomer density $\rho(z) = \mu(z)/(w\sigma)$ is nonnegative

$$\begin{aligned} \mu(z) &= A - Bz^2, \quad z \leq (A/B)^{1/2} \\ &= 0, \quad \text{otherwise} \end{aligned} \qquad (13)$$

with $B = \pi^2/(8N^2a^2)$ determined from eq 11, and $A = (3/2)(\pi^2/12)^{1/3}(w\sigma/a)^{2/3}$ from the normalization of the density, eq 7.

Because $\mu(z)$ is parabolic, $z(s) = z_0 \cos(\pi s/2N)$ for all polymer trajectories. The distribution of the endpoints, z_0, can be found if desired from the fact that it must produce a parabolic density profile. This approximate solution of the SCFT is compared to the exact one in

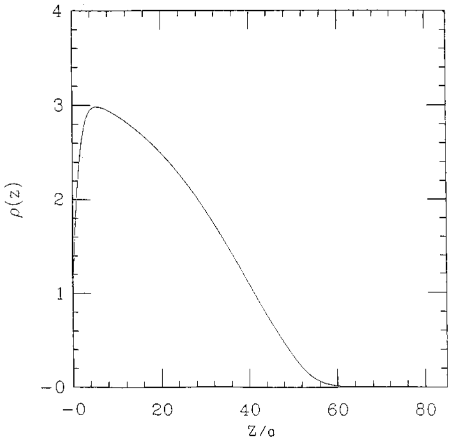

Figure 1. Solution of the self-consistent field equation, eq 5, for $N = 100$ and $w\sigma = 0.1$.

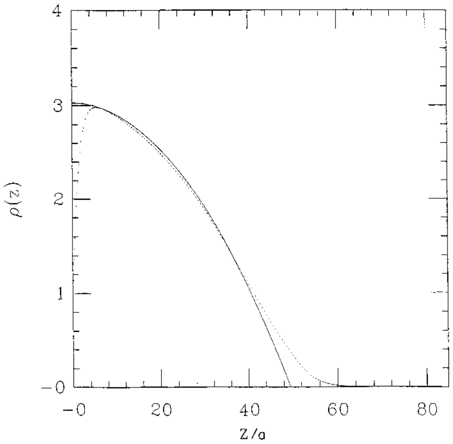

Figure 2. Comparison of the self-consistent field solution and the parabolic profile of eqs 5 and 13 for the same system as in Figure 1.

Figure 2. On the whole, it is quite good. However, just as a classical approximation to a quantum problem is not accurate uniformly over all parts of the trajectory, so the classical approximation above deviates appreciably from the exact solution near the grafting surface and the surface of the brush itself.

The advantages of the approximation lie in its simplicity. It eliminates the labor of calculating the propagator, using only the field variable $\mu(z)$ itself. It also eliminates the element of self-consistency, in that eqs 11 and 12 are solved directly for the field. That the field is related to the density affects the solution for the field *solely* via the requirement that the field must, like the density, be nonnegative. From the solution for the field, the density profile is obtained, and no iterative procedure need be employed to verify that the profile does indeed produce the field.

An alternative approximation to the above which shares with it the virtue that it deals only with the density, and not with the propagator, but which retains the self-consistent nature of the original mean field problem embodied in eq 6 is obtained by expanding the trajectory $z(s)$ in a Fourier series. Since we will impose the grafting condition $z(N) = 0$, it is natural to expand $z(s)$ on a basis of antiperiodic functions, of antiperiod $2N$, so that they vanish at $s = N$. We thus expand:

$$z(s) = \sum_0^\infty \left(z_k \cos\left[\frac{(2k+1)\pi s}{2N}\right] + z'_k \sin\left[\frac{(2k+1)\pi s}{2N}\right]\right) \tag{14}$$

with the constraint $\sum_0^\infty (-1)^k z_k' = 0$, which ensures that $z(N) = 0$.

The approximation to the solution of this equation that we employ is to retain in the Fourier expansion for $z(s)$ only the lowest term, $z_0 \cos(\pi s/2N) + z_0' \sin(\pi s/2N)$. The grafting condition then implies $z_0' = 0$, so that $z(s) = z_0 \cos(\pi s/2N)$, which, as noted above, is the classical solution.

The mean field self-consistent equation (6) becomes

$$\rho(y) = \frac{1}{Q}\int_0^\infty \mathrm{d}z_0 \int_0^N \mathrm{d}s'\, \delta\!\left(y - z_0 \cos\left(\frac{\pi s'}{2N}\right)\right) \exp\left\{-\left(\frac{\pi z_0}{4N^{1/2}a}\right)^2 - w\sigma\int_0^N \mathrm{d}s\, \rho\!\left(z_0 \cos\left(\frac{\pi s}{2N}\right)\right)\right\} \tag{15}$$

where

$$Q = \int_0^\infty \mathrm{d}z_0 \exp\left\{-\left(\frac{\pi z_0}{4N^{1/2}a}\right)^2 - w\sigma\int_0^N \mathrm{d}s\, \rho\!\left(z_0 \cos\left(\frac{\pi s}{2N}\right)\right)\right\} \tag{16}$$

The equation can be made somewhat simpler by carrying out the integral over $\mathrm{d}s'$

$$\int_0^N \mathrm{d}s'\, \delta\!\left(y - z_0 \cos\left(\frac{\pi s'}{2N}\right)\right) = \frac{2N}{\pi({z_0}^2 - y^2)^{1/2}}, \qquad z_0 > y \tag{17}$$

$$= 0, \qquad \text{otherwise} \tag{18}$$

and by rewriting the integral in the exponent

$$\int_0^N \mathrm{d}s\, \rho\!\left(z_0 \cos\left(\frac{\pi s}{2N}\right)\right) = \frac{2N}{\pi}\int_0^{z_0} \frac{\rho(x)\,\mathrm{d}x}{({z_0}^2 - x^2)^{1/2}} \tag{19}$$

so that eqs 15 and 16 become a self-consistent integral equation for the profile $\rho(z)$

$$\rho(y) = \frac{2N}{\pi Q}\int_y^\infty \frac{\mathrm{d}z_0}{({z_0}^2 - y^2)^{1/2}} \exp\left\{-\left(\frac{\pi z_0}{4N^{1/2}a}\right)^2 - \frac{2w\sigma N}{\pi}\int_0^{z_0} \frac{\rho(x)\,\mathrm{d}x}{({z_0}^2 - x^2)^{1/2}}\right\} \tag{20}$$

and

$$Q = \int_0^\infty \mathrm{d}z_0 \exp\left\{-\left(\frac{\pi z_0}{4N^{1/2}a}\right)^2 - \frac{2w\sigma N}{\pi}\int_0^{z_0} \frac{\rho(x)\,\mathrm{d}x}{({z_0}^2 - x^2)^{1/2}}\right\} \tag{21}$$

It is easy to show that this equation produces the scaling $h \sim N(w\sigma a^2)^{1/3}$ provided only that the integral over $\mathrm{d}z_0$ is well approximated by a steepest-descent approximation (*i.e.*, that the classical approximation is justified).

This integral equation is easily solved numerically. In Figure 3, its results are compared to the exact solution of the SCFT for the same values of $N = 100$ and $w\sigma = 0.1$ shown previously. The comparison is very good indeed and is an improvement over the simpler classical form shown in Figure 2. In particular, the distribution at the end of the brush is given quite well. The density is underestimated slightly there because our simple eq 20 overestimates the density near the wall. As the normalizations of the two curves are identical, this excess density is removed from the rest

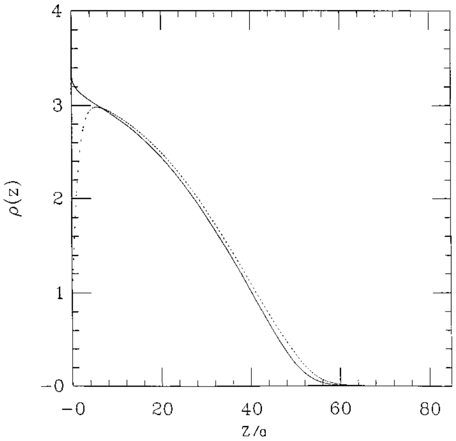

Figure 3. Comparison of the self-consistent field solution and the simplified integral equation eq 20 for the same system as in Figure 1.

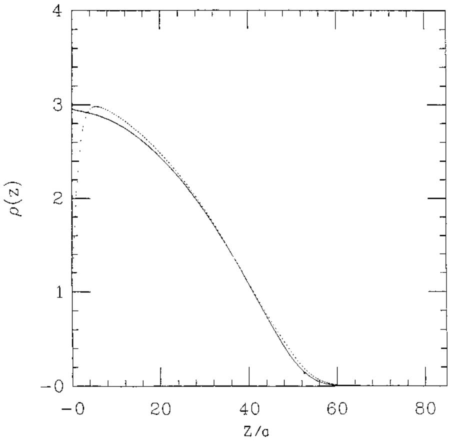

Figure 4. Comparison of the self-consistent field solution and the simplified integral equation eq 32, which contains approximately the effect of the hard wall, for the same system as in Figure 1.

of the distribution. The excess density at the wall can be traced to the fact that we have not at all taken into account the fact that the wall is impenetrable. An approximate treatment of the effect of the hard wall, which is given in the Appendix, leads to an additional factor of z_0 in the integrand of the expression for the single-chain partition function Q. This causes the density at the wall to be reduced, leading to the density profile shown in Figure 4. As can be seen, the main effect is to move the tail of the distribution to larger values of z, but it has had little effect on its *shape*. The shape has been calculated by Witten et al.[18] from the SCFT of eq 8, a linear expansion of the field $\mu(z)$ about the thickness of the parabolic brush $h = (A/B)^{1/2}$, and the assumption of ground state dominance.[19] The result is

$$\rho(z) \propto \exp[-\{(4/3)[(z - h)/\xi]^{3/2}\}] \tag{22}$$

with the characteristic width of the tail

$$\frac{\xi}{h} = \left(\frac{2}{\pi^2}\right)^{1/3}\left(\frac{N^{1/2}a}{h}\right)^{4/3} \tag{23}$$

To show that the profile we have obtained does indeed behave as predicted, we plot in Figure 5 $-\ln(\rho)$ *vs* $[(z - h)/a]^{3/2}$ which correspond to values of z/a from 50 to 100. For the system shown, $h \approx 49.5$. The agreement with the predicted dependence is reassuring, as this form can be obtained without detailed calculation from scaling arguments.[18] It reinforces our conclusion that the simple integral equation, eq 20, captures the essential physics in the outer regions of the brush, and represents an improvement to the simple classical approximation of refs 8−10 in the vicinity of the tail. It is, of course, in this region that the brush interacts most appreciably with its environment, with tail profiles as in Figure 3 leading to weak, long-range repulsions between brushes[17] which are absent in the classical profile. Furthermore, the amount of monomers in the tail region depends on the polymerization index N itself, as seen from eq 23. We therefore expect that if a similar integral equation were used to calculate the phase boundaries between ordered phases of diblock copolymers in the strong segregation limit, a dependence on N would arise which is absent in calculations based on the classical approximation.[7,20] We hope to explore this in the future.

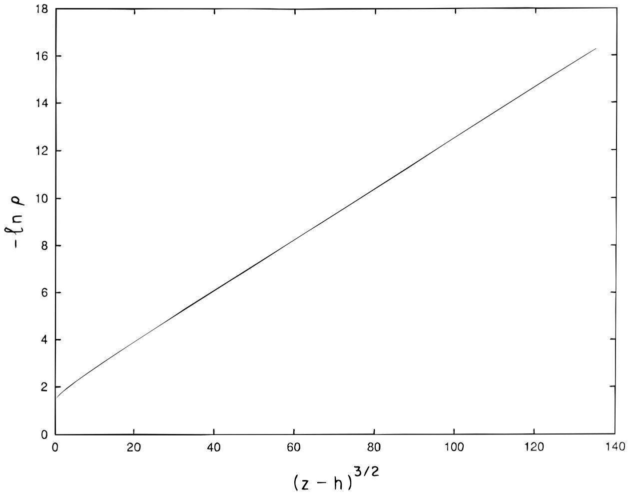

Figure 5. Tail of the distribution produced by the simplified integral eq 20 for the system of Figure 1, for which $h \approx 49.5$. Values of z/a are from 50 to 100. The plot is of a form to show that in this region the monomer density profile behaves as $\exp[-C(z - h)^{3/2}]$, with C a constant.

Acknowledgment. We acknowledge the hospitality of the Institute for Theoretical Physics, Santa Barbara, where this work was initiated. The ITP is supported by NSF Grant No. PHY89-04035. This work was also supported in part by NSF Grant No. DMR9220733.

Appendix

We want to evaluate the partition function, $Q_{hw}(0)$, of a single chain which is anchored to an impenetrable wall located at $z = 0$. Using quantum-mechanical notations, we may write (4) as

$$Q_{\mathrm{hw}}(0) = \int \mathrm{d}z_0 \,\langle 0|\exp(-NH)|z_0\rangle \tag{24}$$

where H is a quantum-like Hamiltonian given by

$$H = -\frac{a^2}{2}\frac{\partial^2}{\partial z^2} + \sigma w \rho(z) \tag{25}$$

Only chain configurations in which no part of the chain is found at negative values of z enter $Q_{\mathrm{hw}}(0)$. We take account explicitly of this restriction by inserting a complete set of states which vanish if the coordinate is equal to the coordinate of the wall. We take the latter to be at $z = -d$, and will take the limit of d to zero. A complete set of states vanishing on the wall at $z = -d$

is provided by the wave functions sin $k(z + d)$, and thus, inserting a projector onto the subspace generated by these wave functions guarantees that the chain cannot penetrate to the left of the wall. Using (4), we may thus write

$$Q_{\mathrm{hw}}(0) = \int \mathrm{d}z_0 \int \frac{\mathrm{d}k}{2\pi} \int_{-d}^{\infty} \mathrm{d}z' \sin kd \sin k(d + z') \langle z' | \exp(-NH) | z_0 \rangle \quad (26)$$

The integration over the wavevector k is carried out, as well as the $d \to 0$ limit, with the result

$$Q_{\mathrm{hw}}(0) = \lim_{d \to 0} [\tilde{Q}_{\mathrm{hw}}(0) - \tilde{Q}_{\mathrm{hw}}(-2d)] \quad (27)$$

where $\tilde{Q}_{\mathrm{hw}}(-2d)$ is a single-chain partition function in which the coordinates of the chain are *not* restricted to remain on the right of the wall. The fact that no part of the chain may enter to the left of the wall is enforced by the subtraction in (27), which is analogous to the image method in elementary electrostatics.

The partition function $\tilde{Q}(0)$ is in fact given in eq 4, where it is denoted $Q[\mu]$. We now expand the trajectories, $z(s)$, as in the text keeping only the first Fourier component. Thus we parameterize the paths appearing in $\tilde{Q}(0)$ as $\tilde{z}(s) \equiv z_0 \cos(\pi s/2N)$ and those appearing in $\tilde{Q}(-2d)$ as $\tilde{z}(s) - 2d \sin(\pi s/2N)$. Therefore

$$\tilde{Q}(0) - \tilde{Q}(-2d) \approx \int \mathrm{d}z_0 \left(\exp\{-\int_0^N \mathrm{d}s\, S[\tilde{z}(s)]\} - \exp\left\{-\int_0^N \mathrm{d}s\, S\left[\tilde{z}(s) - 2d \sin\left(\frac{\pi s}{2N}\right)\right]\right\} \right) \quad (28)$$

where $S[z(s)]$ is the action

$$S[z(s)] = \frac{\dot{z}(s)^2}{2a^2} + \mu(z(s)) \quad (29)$$

With d small, we expand in it to obtain

$$\tilde{Q}(0) - \tilde{Q}(-2d) \approx -2d \int \mathrm{d}z_0 \exp\{-\int_0^N \mathrm{d}s'\, S[\tilde{z}(s')]\} \times \int_0^N \mathrm{d}s \sin\left(\frac{\pi s}{2N}\right) \frac{\delta S[\tilde{z}(s)]}{\delta \tilde{z}(s)} = -\frac{4Nd}{\pi} \times \int \frac{\mathrm{d}z_0}{z_0} \exp\{-\int_0^N \mathrm{d}s'\, S[\tilde{z}(s')]\} \int \mathrm{d}\tilde{z}\, \frac{\delta S[\tilde{z}]}{\delta \tilde{z}} = \frac{4Nd}{\pi} \int \frac{\mathrm{d}z_0}{z_0} \left[\frac{1}{2} \left(\frac{z_0 \pi}{2N} \right)^2 + \mu(z_0) - \mu(0) \right] \times \exp\{-\int_0^N \mathrm{d}s'\, S[\tilde{z}(s')]\} \quad (30)$$

For small values of z_0, we assume for the moment that $\mu(z_0) - \mu(0)$, which by eq 5 is directly proportional to $\rho(z_0) - \rho(0)$, is quadratic in z_0 rather than linear. If so, the square bracket in the integrand is quadratic in z_0, so that, with the other factor of $1/z_0$, the integrand behaves linearly with z_0. For large values of z_0, the integral is dominated by the exponent, so that the specific dependence of the square bracket is unimportant. Finally, realizing that in calculating the normalized density, $\rho(y)$, all constant factors in front of the integral over z_0 cancel, we can take the limit of d to zero, and set constant factors to unity. On carrying out the integral over s' in the exponent, we obtain our approximation

$$Q_{\mathrm{hw}} = \int_0^{\infty} \mathrm{d}z_0\, z_0 \exp\left\{ -\left(\frac{\pi z_0}{4N^{1/2}a} \right)^2 - \frac{2w\sigma N}{\pi} \int_0^{z_0} \frac{\rho(x)\, \mathrm{d}x}{(z_0^{\,2} - x^2)^{1/2}} \right\} \quad (31)$$

from which

$$\rho(y) = \frac{2N}{\pi Q_{\mathrm{hw}}} \int_y^{\infty} \mathrm{d}z_0 \frac{z_0}{(z_0^{\,2} - y^2)^{1/2}} \exp\left\{ -\left(\frac{\pi z_0}{4N^{1/2}a} \right)^2 - \frac{2w\sigma N}{\pi} \int_0^{z_0} \frac{\rho(x)\, \mathrm{d}x}{(z_0^{\,2} - x^2)^{1/2}} \right\} \quad (32)$$

Thus the effect of the hard wall in our approximation is to contribute an extra factor of z_0 to the integrand. The solution of this integral equation for the same system as in previous figures is shown in Figure 4. One sees there that the assumption that the profile is quadratic near the wall is valid except for a very narrow region adjacent to it. As stated in the text, the extra factor of z_0 in the integrand causes the density to be reduced near the wall. The monomers removed from its vicinity must appear further out, which causes the profile to be translated along the positive z axis.

References and Notes

(1) Alexander, S. *J. Phys. (Paris)* **1977**, *38*, 977.
(2) de Gennes, P.-G. *J. Phys. (Paris)* **1976**, *37*, 1443.
(3) Auroy, P.; Auvray, L.; Leger, L. *Macromolecules* **1991**, *24*, 2523.
(4) Edwards, S. F. *Proc. Phys. Soc. London* **1965**, *85*, 613.
(5) Helfand, E.; Wasserman, Z. R. *Macromolecules* **1978**, *11*, 960.
(6) Scheutjens, J. M. H. M.; Fleer, G. J. *J. Phys. Chem.* **1979**, *83*, 1619.
(7) Semenov, A. N. *Sov. Phys.—JETP (Engl. Transl.)* **1975**, *61*, 733.
(8) Milner, S. T.; Witten, T. A.; Cates, M. *Macromolecules* **1988**, *21*, 2610.
(9) Milner, S. T. *Science* **1991**, *251*, 905.
(10) Zhulina, E. B.; Borisov, O. V.; Priamitsyn, V. A. *J. Colloid Interface Sci.* **1990**, *137*, 495.
(11) Dolan, A. K.; Edwards, S. F. *Proc. R. Soc. London* **1975**, *A343*, 427.
(12) Cosgrove, T.; Heath, T.; van Lent, B.; Leermakers, F.; Scheutjens, J. *Macromolecules* **1987**, *20*, 1692.
(13) Chakrabarti, A.; Toral, R. *Macromolecules* **1990**, *23*, 2016.
(14) Murat, M.; Grest, G. *Macromolecules* **1989**, *22*, 4054.
(15) Milner, S. T.; Wang, Z.-G.; Witten, T. A. *Macromolecules* **1989**, *22*, 489.
(16) Carignano, M. A.; Szleifer, I. *J. Chem. Phys.* **1993**, *98*, 5006; *J. Chem. Phys.* **1994**, *100*, 3210.
(17) Martin, J. I.; Wang, Z.-G. *J. Phys. Chem.* **1995**, *99*, 2833.
(18) Witten, T. A.; Leibler, L.; Pincus, P. A. *Macromolecules* **1990**, *23*, 824.
(19) Edwards, S. F. *Proc. Phys. Soc. London* **1965**, *85*, 613.
(20) Semenov, A. N. *Macromolecules* **1994**, *27*, 3103.

MA9508461